PROCEEDINGS OF SCIENCE

# Searches for new physics breaking the *CP* and flavor symmetries in the top quark sector at CMS

**Sergio Sánchez Cruz**[a,*] **on behalf of the CMS Collaboration**

[a] *CERN, European Organization for Nuclear Research*
*Geneva, Swizterland*

*E-mail:* sergio.sanchez.cruz@cern.ch

The top quark plays an important role in a number of new physics models, some of which introduce violations to some of the accidental symmetries of the SM, such as the lepton number conservation or introduce additional sources of others already broken, such as the *CP* symmetry. A set of measurements is presented that probe violation of these symmetries in processes involving the top quark, in association with additional particles.

*The European Physical Society Conference on High Energy Physics (EPS-HEP2025)*
*7-11 July 2025*
*Marseille, France*

*Speaker

 ISSN 1824-8039 . Published by SISSA Medialab.



PoS(EPS-HEP2025)063

## 1. Introduction

In addition to searches for the on-shell production of particles not present in the standard model (SM), the CMS Collaboration [1, 2] is putting forward a program of indirect searches for new physics. These searches instead make use of observables that could be influenced by the presence of particles at a higher energy scale $\Lambda$, beyond the energy reach of the experiment. In this context, the SM effective field theory (SMEFT) [3], an extension of the SM that describes the effect of new particles through additional operators extending the SM Lagrangian, provides a suitable description for the experimental searches. In its most general form, the SMEFT incorporates 2499 additional dimension-6 operators, each associated with a Wilson coefficient (WC). Since a simultaneous measurement of such a number of operators is not yet feasible, additional symmetries are imposed to reduce the number of operators to a manageable level. In the top quark sector, a set of flavor assumptions has been agreed upon in the context of the LHCtopWG [4]. In practice, analyses typically restrict themselves further to a subset of operators by imposing additional assumptions, such as the conservation of the *CP* symmetry and selecting operators that are relevant to a specific topology or final state. In the top quark sector, the most comprehensive analysis so far by CMS probes 26 independent Wilson coefficients (WCs) [5].

However, there is no guarantee that new physics will respect those assumed symmetries. For that reason, the CMS Collaboration is releasing a set of searches in the top quark sector that target specific operators that violate some of these symmetries, such as lepton or baryon number violation [6, 7] or the introduction of flavor-changing neutral currents [8]. In these proceedings, we discuss the two most recent results of this kind released by the CMS Collaboration. The first one is a search for new physics breaking the *CP* symmetry in the associated production of top quarks with a Z boson, and the second one is a search for new physics focusing on interactions involving the Z boson beyond the flavor symmetries discussed in Ref. [4].

## 2. Analysis methodology

Both measurements rely on the estimation of the event yields in a set of categories of interest, designed to obtain sensitivity to different new physics scenarios. The contribution to the event yield introduced by the signals is parametrized as a function of the WCs, which allows to perform inference on the WCs directly from the yields. Signal event yields are estimated using Monte Carlo simulations weighted to reproduce the kinematic properties of different WC scenarios, following the approach described in Ref. [5] and is performed using Monte Carlo simulations with suitable weights to resemble the kinematic properties of scenarios corresponding to different WCs values. The weights can be parametrized as

$$w = w_{\mathrm{SM}} + \sum_i c_i l_i + \sum_{ij} c_i c_j q_{ij}, \tag{1}$$

where $w_{\mathrm{SM}}$ is the SM contribution and the sums run over the WCs. The terms involving $l_i$ ($q_{ij}$) represent the linear (quadratic) contributions to the event weight, which correspond to contribution from the interference between SM and BSM diagrams (from purely BSM contributions). We refer to the former contributions as the "linear" contributions and the latter as the "quadratic" contributions.

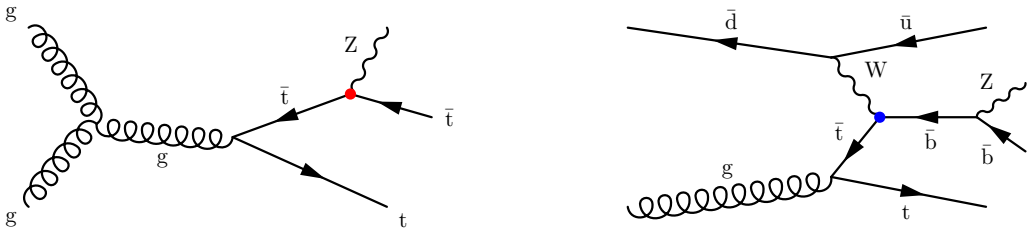


**Figure 1:** Representative diagrams of $t\bar{t}Z$ (left) and tZq production (right). Taken from [9].

In addition to the signal, other processes contribute to the event yield. Events containing at least three leptons produced in the prompt decay of a W or Z boson, or a $\tau$ decay, are estimated using Monte Carlo simulations. Events from other processes, such as $t\bar{t}$ or DY+jets, can contribute to this selection when leptons coming from other sources, such as leptons produced in hadronic jets, are accepted by the identification algorithms. This contribution is estimated by considering events passing the same event selection but where one of the leptons fails the identification criteria, weighted to account for the probability that a non-prompt lepton would have passed the nominal selection criteria.

The signal is extracted by performing a likelihood fit to the observed yields. The likelihood function is built as a product of Poisson probability mass functions with mean equal to the expected number of events. This expectation is modified by the Wilson coefficients, which are determined in the fit, and by a set of systematic uncertainties that are included in the model through a set of nuisance parameters.

## 3. Search for *CP* violation in the production of top quarks associated with Z bosons

The search presented in Ref. [9] searches for $CP$ violation in the associated production of top quarks and Z bosons, using events with three final state leptons, jets, and jets identified as a b jet (b-tagged jets). We use a dataset of proton-proton (pp) collisions collected in 2016–2018 (2022), corresponding to an integrated luminosity of 138 $\text{fb}^{-1}$ (34.7 $\text{fb}^{-1}$) at $\sqrt{s}$ = 13 TeV (13.6 TeV). Events in this selection are dominated by the production of a top quark antiquark pair in association with a Z boson ($t\bar{t}Z$) and the production of a single top quark in association with a Z boson (tZq), which are the signal processes in this search. Some representative diagrams are shown in Fig. 1. Events in this selection also receive contributions from events from WZ and ZZ production, and other minor top quark production processes such as $t\bar{t}W$ or tWZ.

$CP$ violation in this selection can be introduced by the $CP$-odd $c^{I}_{tZ}$ and $c^{I}_{tW}$ operators, defined in Ref. [9], which introduce additional interaction terms between the top quark and the Z boson, affecting the production rate and kinematic properties of $t\bar{t}Z$ and tZq production, respectively. Their effect in other processes contributing to the event yield in this selection was found to be negligible.

Due to the symmetries of $CP$-odd operators, the linear contribution cancels out in any $CP$-even observable, such as the total cross section or standard kinematic variables. For that reason, in order to be sensitive to the linear contribution, we make use of $CP$-odd observables, in which the linear contribution would manifest itself as an antisymmetric contribution to such observables. In contrast, the SM contribution is symmetrically distributed in such observables, and so are the most

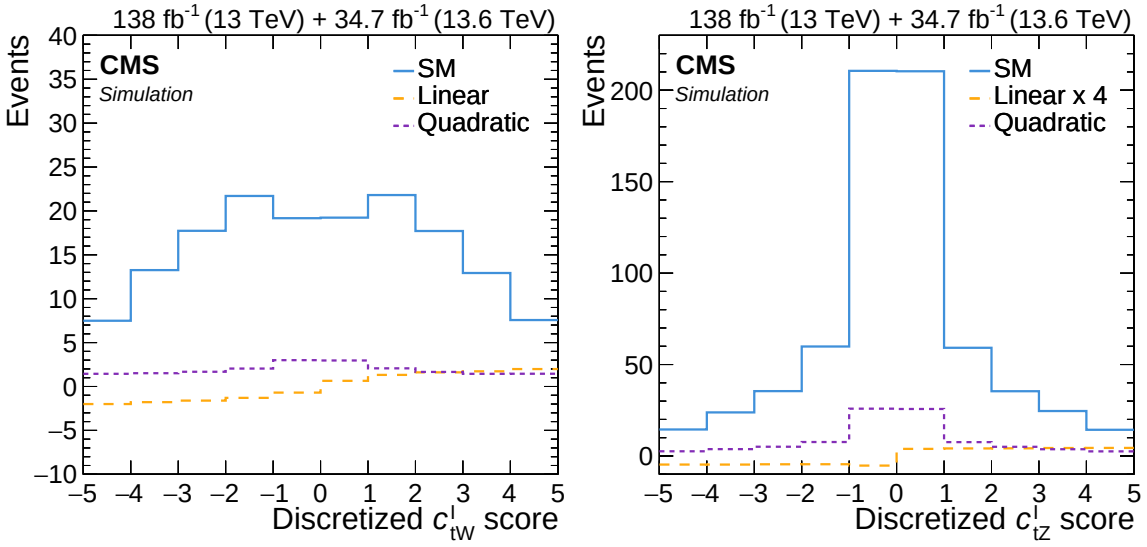


**Figure 2:** Distributions of $g_{c^{I}_{tW}}$ (left) and $g_{c^{I}_{tZ}}$ (right), labeled as discretized score, for tZq and $t\bar{t}Z$ events, respectively. Taken from [9].

systematic uncertainties affecting its prediction. As a consequence, our search is robust against variations in these systematic uncertainties.

In order to optimally extract sensitivity to the operators of interest, we build two *CP*-odd equivariant neural networks [10], $g_{c^{I}_{tW}}$ and $g_{c^{I}_{tZ}}$, one for each of the operators considered. The network architecture is designed in a way that their score is odd under *CP* transformations. As input variables, we use the kinematics of the reconstructed leptons, up to 5 additional jets and missing transverse momentum. The network is parametric as a function of the data taking era to account for the different $\sqrt{s}$ and small changes in detector conditions. The distributions of the neural network scores are shown in Fig. 2 for the signal processes under the SM hypothesis, and the linear and quadratic terms introduced by the operators considered, featuring the symmetry properties described above.

For the signal extraction, events are split in two categories, assigning events with $|g_{c^{I}_{tW}}| > |g_{c^{I}_{tZ}}|$ ($|g_{c^{I}_{tW}}| < |g_{c^{I}_{tZ}}|$ ) to the $c^{I}_{tW}$-like ($c^{I}_{tZ}$-like) category. Events in the $c^{I}_{tW}$-like ($c^{I}_{tZ}$-like) category are further classified as a function of $g_{c^{I}_{tW}}$ ($g_{c^{I}_{tZ}}$). The number of observed events in bins of the two distributions are shown in Fig. 3 along with the prediction obtained by fixing all the parameters to the value observed in the fit. Good agreement is observed between data and the prediction for the $c^{I}_{tW}$ score in the $c^{I}_{tW}$-like region, while a slight excess and an asymmetry are observed in the $c^{I}_{tZ}$ score in the $c^{I}_{tZ}$-like region.

Figure 4 shows the limits as a function of $c^{I}_{tW}$ and $c^{I}_{tZ}$ for scenarios assuming the presence of linear contributions only and linear and quadratic contributions together. The results in both scenarios are consistent with the SM within two standard deviations. The largest discrepancy is observed in $c^{I}_{tZ}$ where data favors positive values, with an observed local significance of 2.5 standard deviations relative to the SM hypothesis, when only linear terms are considered. The discrepancy is driven by the slight asymmetry observed in the $g_{c^{I}_{tZ}}$ distribution.

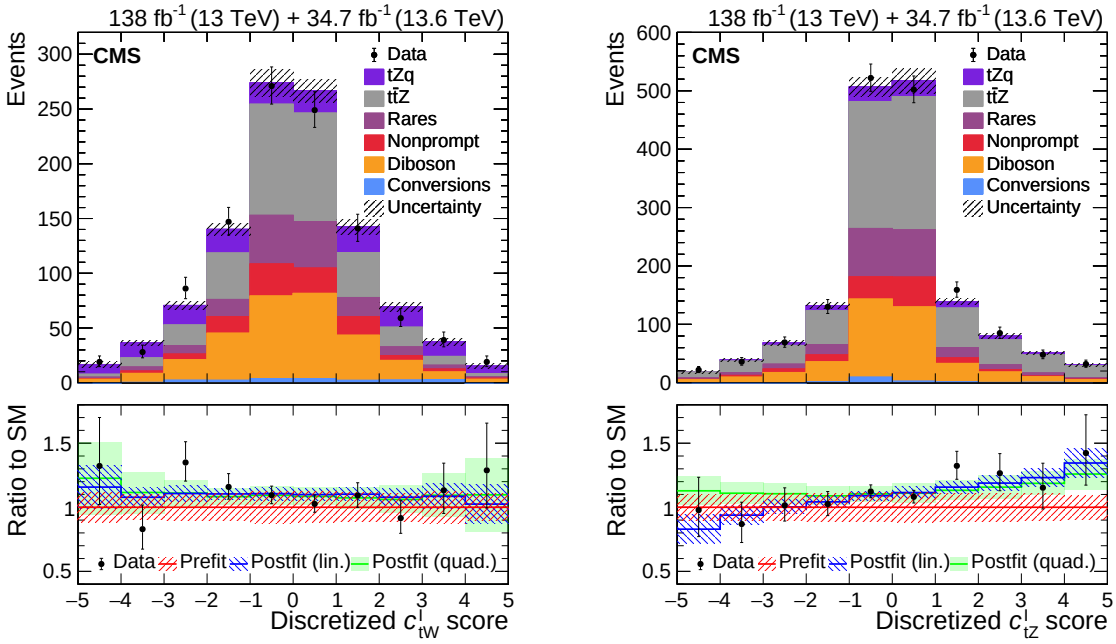


**Figure 3:** Distributions of $g_{c^{I}_{tW}}$ (left) and $g_{c^{I}_{tZ}}$ (right) in the $c^{I}_{tW}$-like and $c^{I}_{tZ}$-like regions, respectively. Taken from [9].

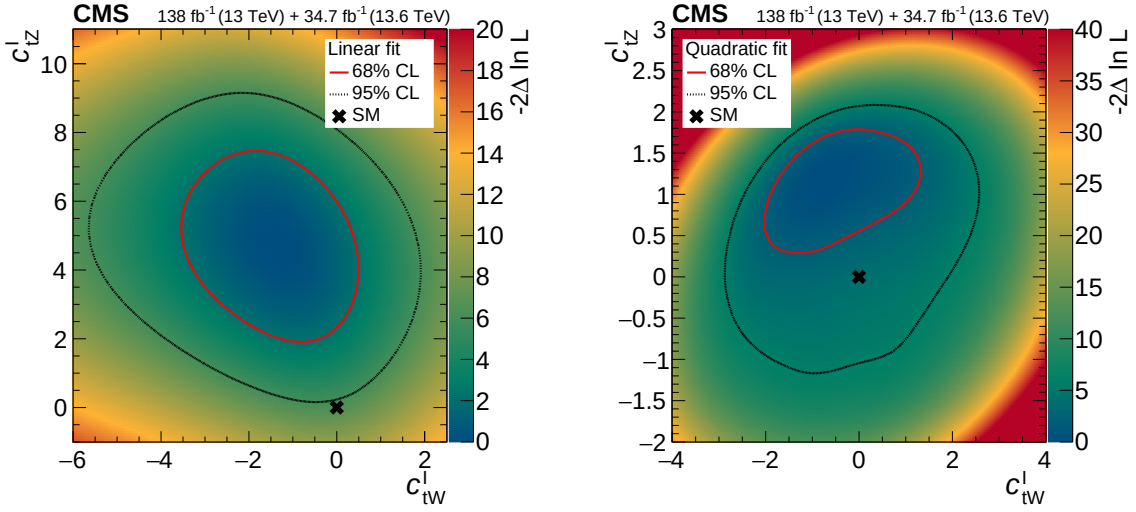


**Figure 4:** Likelihood scans as functions of $c^{I}_{tW}$ and $c^{I}_{tZ}$, including linear contributions only (left) and both linear and quadratic contributions (right). Taken from [9].

## 4. Flavor structure of dimension-6 EFT operators in multilepton final states

Reference [11] describes a complementary search for new physics in the multilepton final state, using a dataset of pp collisions collected in 2016–2018 at $\sqrt{s}$ = 13 TeV, using events with at least three leptons including a Z boson decay candidate.

The analysis explores a subset of operators that modify the interactions between Z bosons and quarks: $O_{\varphi q}^{(-)(ab)}$, $O_{\varphi q}^{(3)(ab)}$, $O_{\varphi u}^{(ab)}$, $O_{\varphi d}^{(ab)}$, along with another two that modify the WZ vertex, namely $O_W$ and $O_{\widetilde{W}}$. The $a$ and $b$ indices denote the indices of the generations affected by the operator. This analysis takes into account, for the first time, operators affecting different generations simultaneously. In particular, this analysis considers the associated Wilson coefficients $c_{\varphi q}^{(3)(11+22)}$, $c_{\varphi q}^{(3)(33)}$, $c_{\varphi q}^{(-)(11+22)}$, $c_{\varphi q}^{(-)(33)}$, $c_{\varphi u}^{(11+22)}$, $c_{\varphi u}^{(33)}$, $c_{\varphi d}^{(11+22)}$, $c_{\varphi d}^{(33)}$, $c_W$, and $c_{\widetilde{W}}$. Operators labeled with 33 in the superindex introduce modifications in the interactions between the top quark and the Z boson, affecting the production rate and kinematic properties of $t\bar{t}Z$ production. Operators labeled $11 + 22$ modify couplings with the first and second generation quarks, affecting the production rate and kinematics of $t\bar{t}Z$ but also diboson processes such as WZ and ZZ. The $c_W$ and $c_{\widetilde{W}}$ coefficients modify the WZ and ZZ interactions and therefore affect the production rate and kinematics of WZ and ZZ production. All the processes mentioned contribute to the event yield in the selection used in the analysis so we perform a simultaneous measurement of all the operators.

To gain additional sensitivity, events are categorized in three regions labeled as $t\bar{t}Z$, WZ and ZZ regions. In addition to the requirements indicated above, events in the $t\bar{t}Z$ region are required to have no additional leptons, at least three jets and at least one b-tagged jet. To build the WZ region, we require instead the missing transverse momentum to be larger than 60 GeV and no jet identified as b-quark jet. Events in the ZZ region are required to contain at least four leptons forming two Z boson candidates. Events are further classified according to the $p_{\mathrm{T}}$ of the leading Z boson candidate.

The effects of the operators on the production rate and Z boson candidate $p_{\mathrm{T}}$ distribution are shown in Fig. 5. It shows that the $t\bar{t}Z$ process is sensitive to third generation couplings, while WZ and ZZ production are sensitive to the couplings of light quarks to the Z bosons. The observed distributions are also shown in Fig. 5. Compared to the SM prediction, the WZ and ZZ cross sections are measured to be 5% lower and 10% higher, respectively.

Figure 6 summarizes the observed WC limits, both individually and in a simultaneous fit. The slight discrepancies in the WZ and ZZ normalization drive small discrepancies of the $c_{\varphi q}^{(3)(33)}$ and $c_{\varphi q}^{(3)(11+22)}$ operators but are still within two standard deviations of the SM values. Besides that, all results are consistent within one standard deviation with the SM value.

## 5. Summary

These proceedings discussed the two most recent results from the CMS Collaboration on indirect searches for new physics that break the $CP$ and flavor symmetries. No significant deviations were reported with respect to the SM prediction. These measurements are still dominated by the limited sizes of the LHC Run 2 and early Run 3 datasets, and are therefore expected to become more sensitive as larger datasets are collected and analyzed.

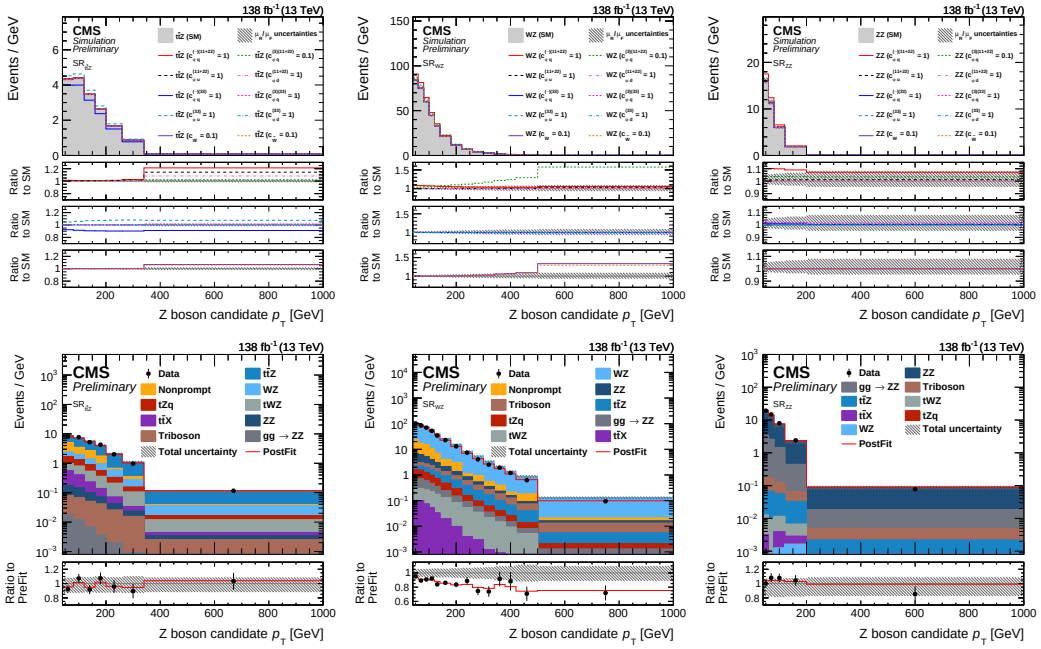


**Figure 5:** Upper row: Distribution of the Z boson candidate $p_T$ for $t\bar{t}Z$ (left), WZ (middle), and ZZ (right) simulated events, each in its corresponding region. The SM prediction is shown along the prediction for different BSM scenarios. Lower row: Observed and simulated distributions of the Z boson candidate $p_T$ in the $t\bar{t}Z$ (left), WZ (middle), and ZZ (right) regions. Taken from [11].

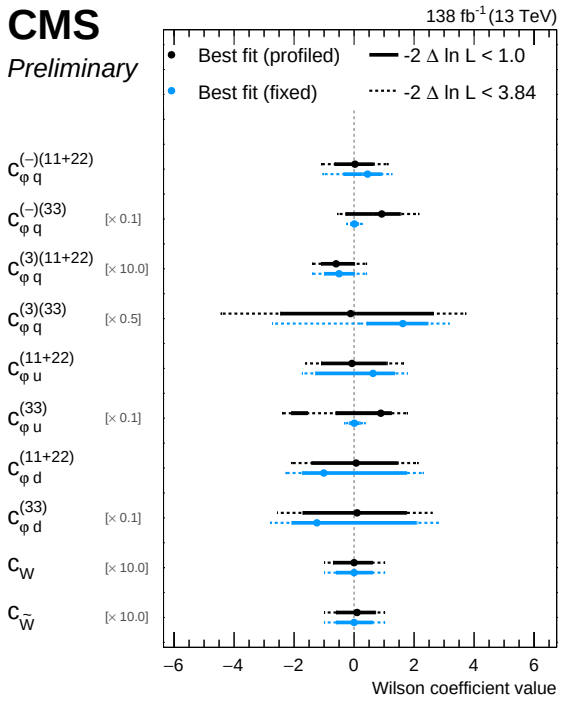


**Figure 6:** Observed limits on the Wilson coefficients of interest. Taken from [11].

## References

[1] CMS Collaboration, *JINST* **3** S08004 (2008)

[2] CMS Collaboration, *JINST* **19** P05064 (2024)

[3] CMS Collaboration, *Annals Phys.* 335 (2013) 21

[4] J. A. Aguilar Saavedra et al., *arXiv:1802.07237*

[5] CMS Collaboration, *JHEP* 12 (2023) 068

[6] CMS Collaboration, *PRL* 132 (2024) 241802

[7] CMS Collaboration, *LFV* 111 (2025) 012009

[8] CMS Collaboration, *PRD* 109 (2024) 072004

[9] CMS Collaboration, *PLB* 869 (2025) 139857

[10] S. Sánchez Cruz et al., *PRD* 110, 096023 (2024)

[11] CMS Collaboration, *CMS-PAS-TOP-23-009*